ELSEVIER

Chemical Geology 192 (2002) 289–306

CHEMICAL GEOLOGY
INCLUDING
ISOTOPE GEOSCIENCE

www.elsevier.com/locate/chemgeo

Allanite: thorium and light rare earth element carrier in subducted crust

Jörg Hermann*

Research School of Earth Sciences, The Australian National University, 0200 ACT Canberra, Australia

Received 13 February 2002; accepted 5 August 2002

Abstract

The investigation of deeply subducted eclogites from the Dora-Maira massif, Western Alps reveals that accessory minerals are important hosts for trace elements. Rutile contains most of the bulk rock Ti, Nb and Ta while zircon hosts nearly all Zr and Hf. More than 90% of the bulk rock light rare earth elements (LREE) and Th and about 75% of U are incorporated in accessory allanite. Phengite is the most interesting major mineral because it hosts more than 95% of Rb, Ba and Cs. Synthesis piston cylinder experiments in a model crustal composition in the range 2.0–4.5 GPa, 680–1150 °C doped with trace elements demonstrate that accessory allanite forms at the expense of the major mineral zoisite at temperatures above 700 °C and 2.0 GPa. Allanite is stabilised by the incorporation of light rare earth elements and was found up to temperatures of 1050 °C and to pressures of at least 4.5 GPa. Disappearance of allanite is caused by dissolution in a coexisting hydrous granitic melt and is not related to the breakdown of any major phase. Experimentally determined element partitioning between allanite and a hydrous granitic melt at 900 °C, 2.0 GPa yield $D_{\mathrm{LREE}}^{\mathrm{all/melt}}$ of about 200, $D_{\mathrm{Th}}^{\mathrm{all/melt}}$ of 60 and $D_{\mathrm{U}}^{\mathrm{all/melt}}$ of 20. These results, combined with literature data, are used to estimate light rare earth element saturation levels of subduction zone liquids as a function of temperature. Allanite is a residual phase up to temperatures of at least 900 and 1000 °C for metabasalts and metasediments, respectively, at $\leq 10\%$ partial melting. Allanite is therefore capable of controlling LREE and to a lesser extent Th contents for the critical temperature range of subduction zone liquid extraction. Low temperature fluids coexisting with allanite are not capable of transporting significant amounts of light rare earth elements and therefore arc lavas showing enrichment of these elements probably originate from a mantle source that experienced metasomatism by a hydrous granitic melt.
© 2002 Elsevier Science B.V. All rights reserved.

Keywords: Allanite; Experimental petrology; Eclogite; Subduction; Trace elements

1. Introduction

Allanite is an epidote-group mineral, which can incorporate weight percents of the light rare earth elements (LREE) La, Ce and Nd as well as Th (Exeley, 1980; Brooks et al., 1981; Gromet and Silver, 1983). Allanite is an important accessory mineral in granites where its influence on trace element evolution is well known (Gromet and Silver, 1983; Sawka et al., 1984). Much less investigated is the role metamorphic allanite may play in subduction zone processes. LREE and Th are important elements for the characterisation of the subduction component in arc lavas (McCulloch

* Tel.: +61-2-6125-8842; fax: +61-2-6125-5989.
E-mail address: Joerg.Hermann@anu.edu.au (J. Hermann).

0009-2541/02/$ - see front matter © 2002 Elsevier Science B.V. All rights reserved.
PII: S0009-2541(02)00222-X

and Gamble, 1991; Pearce and Peate, 1995; Elliott et al., 1997; Hawkesworth et al., 1997). Therefore, a profound understanding of the behaviour of these elements in subduction zone processes is only possible if we know in which phases LREE are incorporated, how stable these phases are and how they interact with subduction zone liquids. Allanite has been described from high-pressure garnet-amphibolites (Sorensen, 1991), eclogites (Tribuzio et al., 1996) as well as high-pressure gneisses (Carswell et al., 2000). While these field-based studies indicate that allanite could be stable up to 2.5 GPa, no detailed experimental data on the high-pressure stability of allanite is available yet. Tribuzio et al. (1996) determined that about 60% of the bulk rock LREE in an eclogite were hosted in allanite. This indicates that allanite has the potential to be a major carrier of LREE and Th in subducted crustal material.

In this paper, the importance of allanite for subduction zone processes is revealed using experimental petrology, metamorphic petrology and trace element geochemistry. Bulk rock and mineral trace element data from deeply subducted eclogites containing allanite are used to determine the LREE and Th budget in subducted crustal material. The stability of allanite is experimentally determined in the range from 2.0 to 4.5 GPa and 680 to 1150 °C in a model crustal composition. Additionally, experimental REE, Th and U partitioning between allanite and a hydrous granitic melt at 900 °C and 2.0 GPa is presented. The experimental data is combined with literature data in order to obtain information on the LREE saturation of subduction zone liquids. This information is used to establish the influence of allanite on the composition of subduction zone liquids.

2. Experimental and analytical techniques

Synthesis experiments were run in end-loaded 1.27 cm piston-cylinder apparatuses. Pressure was calculated from direct conversion of load to pressure in the low friction experiments using salt sleeves and Teflon foil and is accurate to ±0.1 GPa. Temperature was controlled using type B thermocouples ($Pt_{94}Rh_6/Pt_{70}Rh_{30}$) and is accurate to ±10 °C. The starting material P1 was prepared with the sol–gel technique (Luth and Ingamells, 1965) in order to homogenise the selected trace elements and was then fused to a glass at 1400 °C, 1 atm for 20 min. Details about the preparation of starting material and experimental procedure are given by Hermann and Green (2001) and Hermann (2002). In order to produce allanite coexistent with a hydrous granitic liquid in a natural system, a LREE-rich granodioritic starting material was prepared (ZG1). A silica-rich trace element mix was prepared by the sol–gel technique with all ingredients except Ca, Mg, Fe, and Al. Fe was added as fayalite, Ca as oxide, Al and Mg as hydroxides (H_2O source). Fifteen milligrams of the starting material was loaded in an $Ag_{50}Pd_{50}$ capsule, which was closed by arc welding under an Argon gas stream.

Experimental phase relations were examined in polished sections of the capsules by backscattered electron images on a JEOL 6400 SEM (Electron Microscopy Unit, ANU). The phase compositions of experimental runs and natural samples were determined using an energy dispersive detector, an acceleration voltage of 15 kV and a beam current of 1 nA. Natural samples were also analysed with a Camebax Electron Microprobe using an acceleration voltage of 15 kV and a beam current of 6 nA. The LREE content of some allanites was determined by wave dispersive spectrometry (WDS) with a Camebax Electron Microprobe using an acceleration voltage of 25 kV and a beam current of 30 nA. Because interference problems in WDS-analyses of REE-rich materials can severely affect the result, the large allanite analysed with Laser Ablation ICP-MS of experiment C-1245 was used for standardisation to account for LREE overlap.

Bulk rock major elements and some trace elements were determined with standard XRF and solution ICP-MS techniques at the Australian Geological Survey Organisation (now Geoscience Australia, for information see: http://www.ga.gov.au.). To completely dissolve accessory minerals, the rock powders were first fused to a glass with a flux of lithium tetraborate and lithium metaborate and then dissolved in a mixture of HF and HNO_3. For further trace element analyses, the devolatilised rock powders were fused with a lithium–metaborax flux in the ratio 2:1 at 1200 °C for 20 min to form a glass. To determine bulk rock Li and B contents, the rock powders were fused on a molybdenum-strip under an argon pressure of a few bars. The

trace element contents of the glasses and of minerals in thin section were analysed by Laser Ablation—ICP-MS at the Research School of Earth Sciences (Eggins et al., 1998). A pulsed 193 nm ArF Excimer laser with 100 mJ energy at a repetition rate of 5 Hz was used for ablation. Sample DM 9 (apart from apatite and zircon) was analysed on a Perkin-Elmer Sciex ELAN 6000 ICP-MS. The bulk rock glasses and the other minerals were analysed on an Agilent 7500 quadrupole ICP-MS. Two batches of analyses were used to determine the trace elements of the glasses and the minerals in sample DM 9. Spot sizes for mineral analysis were between 170 and 23 μm. During the time-resolved analysis of minerals, the contamination from inclusions, fractures and zones of different composition was detected by monitoring several elements and integrating only the 'clean' part of the signal. The relative 1σ standard deviation of multiple mineral analyses is generally about 5–20%. A NIST-612 glass was used as standard material and values were taken form Pearce et al. (1997).

3. Allanite in deeply subducted eclogites

Accessory allanite was found in two phengite eclogites from the Dora-Maira massif (Western Alps). The Dora-Maira massif is a slice of continental crust that was subducted to 3.7–4.3 GPa and experienced peak metamorphic temperatures of about 730 °C during Alpine convergence (Schertl et al., 1991; Hermann, in press). The eclogites form meter thick-layers within metapelites. The bulk rock trace element composition is characterised by high LREE and high field strength element (HFSE) contents and intermediate large ion lithophile element (LILE; Table 1). This suggests that the protoliths of the eclogite layers were alkaline mafic rocks.

The rocks contain garnet, omphacite, quartz (probably pseudomorph after coesite), phengite, rutile and accessory allanite, apatite and zircon. Allanite displays straight grain boundaries with the major eclogite facies minerals (Fig. 1), indicating that it was stable during peak metamorphic conditions. The major element compositions of the rock-forming minerals and allanite are given in Table 2.

The importance of allanite in trace element budgets of subducted crust is evaluated from mass balance.

Table 1
Major and trace element contents of two phengite eclogites from the Dora-Maira Massif, Western Alps

wt.%	DM 9	DM 30
SiO_2	50.09	54.69
TiO_2	2.43	2.53
Al_2O_3	14.87	15.04
FeO	12.27	10.09
MnO	0.15	0.17
MgO	6.52	4.86
CaO	9.82	7.70
Na_2O	2.71	2.91
K_2O	0.66	1.22
P_2O_5	0.27	0.22
SO_3	0.05	0.04
Total	99.84	99.47
ppm		
Li[c]	102	46
Be[b]	1.8	1.1
B[c]	12	11
F[a]	650	599
Cl[a]	117	6
Sc[a]	24	34
V[a]	210	279
Cr[a]	425	47
Co[c]	47	25
Ni[a]	232	11
Cu[a]	33	23
Zn[a]	131	82
Ga[b]	19	18
Ge[b]	2.0	1.7
As[a]	0.8	1.5
Br[a]	2	1
Rb[a]	33	55
Sr[a]	176	128
Y[c]	27	40
Zr[c]	252	159
Nb[c]	40	12
Mo[b]	0.7	0.8
Cd[b]	0.19	0.15
Sn[b]	3.7	4.7
Sb[b]	0.3	0.1
Cs[b]	1.2	1.68
Ba[c]	108	107
La[c]	52	23
Ce[c]	101	47
Pr[c]	11.4	6.2
Nd[c]	44	26
Sm[c]	7.9	6.2
Eu[c]	2.2	1.7
Gd[c]	7.4	6.9
Tb[c]	1.0	1.1
Dy[c]	5.8	6.9
Ho[c]	1.0	1.4
Er[c]	2.8	3.9

(continued on next page)

Table 1 (*continued*)

wt.%	DM 9	DM 30
ppm		
Tm[c]	0.38	0.56
Yb[c]	2.6	3.7
Lu[c]	0.37	0.53
Hf[c]	6.0	4.0
Ta[c]	2.60	0.94
Pb[b]	10	3.7
Bi[b]	0.2	0.1
Th	[b]9.1	[c]5.4
U	[b]1.9	[c]1.4

The major and the trace elements annotated with [a] were measured by XRF. [b] and [c] refer to trace element analyses by solution and Laser Ablation ICP-MS, respectively.

Allanite contains several wt.% of LREE, about 1 wt.% Sr, more than 5000 ppm Th and about 1000 ppm of U and Pb (Table 3). The chondrite-normalised REE pattern of allanite displays a strong enrichment of LREE with respect to HREE (Fig. 2). Apatite is the second richest phase in LREE (Fig. 2). However, the distribution coefficient $D_{La}^{all/apa}$ is about 550, indicating that these elements strongly prefer allanite. Zircon is the second richest phase in Th but $D_{Th}^{all/zir}$ is still about 100. Garnet and omphacite display LREE-depleted patterns (Fig. 2) and phengite and rutile are at or below detection limit for the REE.

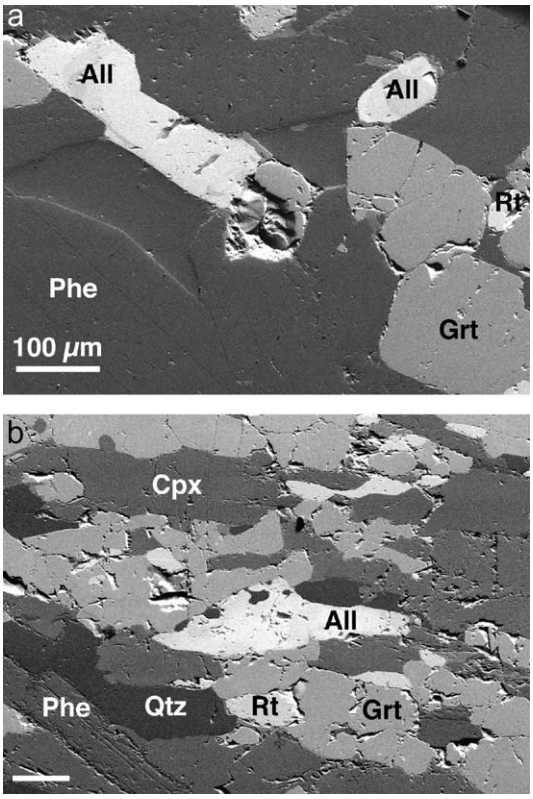

Fig. 1. Backscattered electron images of allanite in phengite eclogites. Allanite (All) coexists with phengite (Phe), garnet (Grt) and rutile (Rt) in sample DM 9 (a). Allanite forms part of the high-pressure foliation together with omphacite (Cpx), quartz (Qtz), garnet and rutile in sample DM 30 (b). Scale bars are 100 μm.

Table 2
Representative electron microprobe mineral analyses from the phengite eclogites

Sample	DM 9				DM 30			
mineral	Grt	Cpx	Phe	All	Grt	Cpx	Phe	All
SiO_2	38.5	56.42	51.35	33.15	39.29	57.67	51.68	33.10
TiO_2	<0.07	<0.07	0.42	0.31	<0.07	<0.07	0.41	0.08
Al_2O_3	21.95	12.47	24.17	22.46	22.14	13.42	25.43	20.78
FeO	24.29	3.04	1.61	6.24	23.60	2.94	1.72	6.57
MnO	0.26	<0.08	<0.08	<0.08	0.50	<0.08	<0.08	0.25
MgO	5.16	7.69	4.17	0.17	5.71	7.45	3.93	0.10
CaO	11.11	12.72	<0.06	15.99	10.16	11.81	0.22	15.21
Na_2O	<0.15	7.64	<0.15	<0.15	<0.15	8.15	<0.15	<0.15
K_2O	<0.04	<0.04	11.17	<0.04	<0.04	<0.04	10.81	<0.04
Total	101.27	99.98	92.89	78.32	101.42	101.46	94.20	76.09

The amount of each phase and its contribution to the trace element budget in the eclogites are obtained from mass balance using bulk rock and mineral data (Fig. 3). The results demonstrate that the major minerals garnet (35–40% abundance) and clinopyroxene (35–40%) host only fractions of the trace elements. Garnet accounts for more than 90% of Y and the HREE and contributes significantly to the budget of MREE. Clinopyroxene hosts more than 95% of Na and Li and contains significant amounts of Be and transition metals such as V. About 40% of Pb and 50% of Sr, but insignificant amounts of REE and HFSE are found in clinopyroxene. Phengite is the most interesting major mineral because it is the main host of the LILE, in agreement with the previous studies on phengite bearing high pressure rocks (Domanik et al., 1993; Sorenson et al., 1997; Zack et al., 2001). While phengite contains the highest amount of B and Be, due to its lower abundance with respect to omphacite it contributes only to 20% and 10% of the bulk rock, respectively. It is expected that in subducted sediments, where the amount of phengite exceeds omphacite, phengite is

Table 3
Average trace element contents of multiple mineral analyses from the phengite eclogite determined with LA ICP-MS (n.a. = not analysed)

	DM 9							DM 30						
	Cpx (6)	Grt (6)	Phe (5)	All (5)	Rut (5)	Apa (4)	Zir (2)	Cpx (7)	Grt (6)	Phe (7)	Alla (7)	Rut (4)	Apa (6)	Zir (6)
Li	369	< 3.86	93.4	11.3	< 3.86	< 0.898	< 10.2	117	2.13	14.6	4.88	< 2.01	< 2.01	< 10.2
Be	3.83	< 2.12	4.15	< 2.12	< 2.12	< 0.310	< 3.62	3.03	< 0.170	2.69	< 0.769	< 0.769	< 0.769	< 3.62
B	11.2	< 7.62	40.7	< 7.62	< 7.62	12.1	< 10.2	14.5	6.46	37.8	8.20	3.22	9.16	< 10.2
P	< 21.2	164	23.9	587	< 21.2	179,015[a]	652	14.6	63.3	14.5	243	7.18	179,015[a]	429
Sc	11.2	55.4	1.39	13	1.63	0.148	566	19.5	79.5	2.67	21.5	1.96	0.073	413
Ti	544	342	2812	821	593,300[a]	21.7	2145	401	273	2517	976	593,300[a]	14.0	2156
V	352	73	211	457	1077	0.168	3.56	383	59.8	242	431	1294	0.161	0.882
Cr	319	247	312	278	636	n.a.	n.a.	n.a.	n.a.	n.a.	n.a.	n.a.	n.a.	n.a.
Mn	99	2560	9.8	138	173	n.a.	n.a.	n.a.	n.a.	n.a.	n.a.	n.a.	n.a.	n.a.
Co	25.7	62	18	22	0.45	n.a.	n.a.	n.a.	n.a.	n.a.	n.a.	n.a.	n.a.	n.a.
Ni	233.8	6.61	276	85	0.34	n.a.	n.a.	n.a.	n.a.	n.a.	n.a.	n.a.	n.a.	n.a.
Zn	173	187	127	280	17.2	n.a.	n.a.	n.a.	n.a.	n.a.	n.a.	n.a.	n.a.	n.a.
Ga	34.6	12.8	70.4	124	0.95	n.a.	n.a.	n.a.	n.a.	n.a.	n.a.	n.a.	n.a.	n.a.
Ge	1.06	3.94	0.43	21.3	0.23	n.a.	n.a.	n.a.	n.a.	n.a.	n.a.	n.a.	n.a.	n.a.
Rb	< 1.110	< 1.110	488	< 1.110	< 3.110	0.057	< 0.304	< 0.012	< 0.153	482	< 0.053	< 0.053	< 0.053	0.534
Sr	153	2.2	140	11,838	n.a.	3567	0.66	127	0.416	99.1	9835	n.a.	4738	0.678
Y	0.290	57.56	< 0.095	40.9	< 1.36	34.7	576	0.541	89.8	0.306	52.6	0.141	58.9	1498
Zr	1.48	1.28	< 0.204	2.88	98.5	0.032	488,570[a]	0.871	1.03	0.132	1.66	92.1	0.03	488,570[a]
Nb	< 0.096	< 0.096	1.39	< 0.543	1373	0.021	1.72	< 0.006	< 0.006	0.401	0.062	453	< 0.027	0.821
Cs	< 0.177	< 0.177	15.4	< 0.177	< 4.01	< 0.042	< 0.443	< 0.017	< 0.017	14.5	< 0.077	< 0.077	< 0.077	< 0.443
Ba	< 0.650	0.858	1512	214	< 1.43	0.86	< 1.04	< 0.038	< 0.255	886	10.8	< 0.174	0.313	< 1.04
La	0.254	< 0.053	< 0.053	27,552	< 0.912	46.4	< 0.160	0.066	< 0.006	0.067	24,373	< 0.026	46.4	< 0.160
Ce	0.733	0.131	< 0.032	51,144	< 0.652	174	1.65	0.342	0.074	0.007	53,878	< 0.034	216	16.0
Pr	0.161	0.155	< 0.018	5514	< 0.402	33.8	< 0.131	0.105	0.073	0.021	6297	< 0.022	49.9	0.164
Nd	0.942	1.20	< 0.041	16,833	< 1.12	221	0.28	0.831	0.951	0.087	23,816	< 0.083	372	2.79
Sm	0.533	2.18	< 0.107	2419	< 2.49	88.2	0.798	0.529	3.39	0.026	3169	< 0.085	169	5.61
Eu	0.182	1.94	< 0.033	476	< 0.728	18.8	0.223	0.161	2.25	0.016	454	< 0.046	37.6	0.720
Gd	0.384	7.76	< 0.008	625	< 0.184	80.7	6.28	0.466	12.6	0.043	753	< 0.177	129	30.4
Tb	0.045	2.01	< 0.039	27	< 0.563	5.59	2.72	0.042	2.50	< 0.011	26.8	< 0.049	8.39	10.7
Dy	0.115	13.8	< 0.071	37.7	< 1.170	14.9	42.6	0.175	16.7	0.047	41.7	< 0.088	23.1	132
Ho	< 0.017	2.70	< 0.017	1.91	< 0.285	1.34	18.6	0.021	3.33	0.010	2.51	< 0.019	2.22	48.5
Er	< 0.036	6.96	< 0.036	1.63	< 0.725	1.97	108	0.043	9.54	0.029	4.41	< 0.083	3.19	222
Tm	< 0.015	1.09	< 0.015	0.081	< 0.204	0.17	28.4	0.005	1.36	0.005	0.162	< 0.022	0.251	44.6
Yb	< 0.038	7.14	< 0.038	0.326	< 0.619	0.805	359	0.029	9.08	0.024	0.701	< 0.061	1.05	417
Lu	< 0.010	1.14	< 0.010	0.036	< 0.202	0.106	68	< 0.007	1.27	< 0.007	0.067	< 0.023	0.106	69.7
Hf	0.124	< 0.028	< 0.028	0.094	4.03	< 0.042	9874	0.084	0.018	0.028	0.078	3.90	< 0.078	7594
Ta	< 0.010	< 0.010	0.064	< 0.437	83.5	< 0.019	1.36	< 0.008	< 0.008	0.012	< 0.036	38.3	< 0.036	0.503
Pb	6.94	0.468	18.8	1377	< 1.82	32.4	3.87	3.76	0.686	9.81	840	0.146	29.2	11.8
Th	< 0.016	< 0.016	< 0.016	5164	< 0.286	0.576	55.8	< 0.007	< 0.007	< 0.007	5424	< 0.033	1.46	449
U	0.008	0.041	0.011	951	0.831	1.52	507	0.016	0.027	0.026	1165	1.86	6.43	624

[a] Converted from major element analysis.

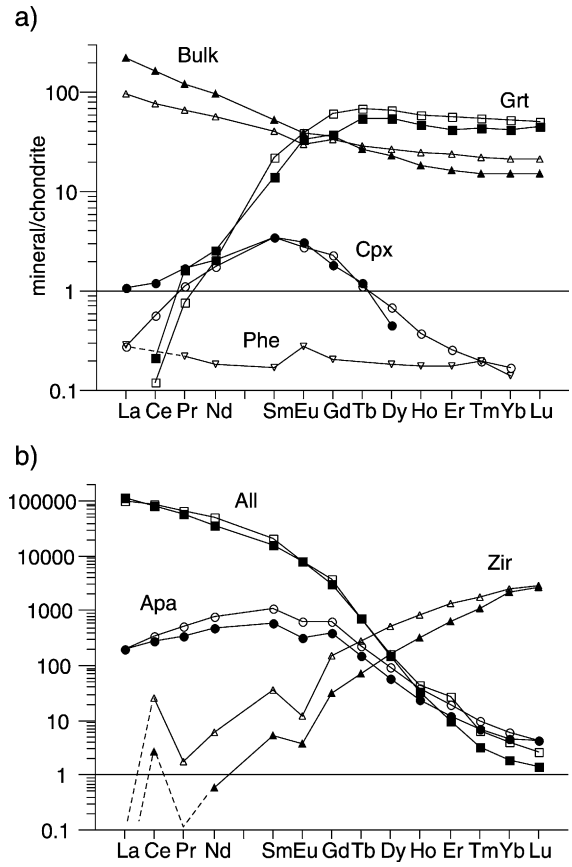

Fig. 2. Chondrite-normalised (Sun and McDonough, 1989) REE patterns of bulk rocks major minerals (a) and accessory minerals (b) of sample DM 9 (filled symbols) and DM 30 (open symbols). The REE content of rutile is below the detection limit.

the most important carrier for Be and B. Rutile contains more than 95% of bulk Ti, Nb and Ta. This is in agreement with previous work showing that rutile is the major host of these elements in subducted mafic rocks (Rudnick et al., 2000; Zack et al., 2002). Although the abundance of allanite is only 0.1–0.2% it contains more than 95% of La, Ce and Pr and more than 90% of Nd. Moreover, allanite hosts about 75% of U and almost all Th. Apatite dominates the P-budget and contributes with 10–20% to the total amount of Sr and MREE. Finally, zircon hosts nearly all Zr and Hf and about 10–15% of U. In summary, the trace element distribution from a deeply subducted eclogite demonstrates that accessory allanite is the most important host for LREE, Th and to a lesser extent U. Allanite is part of the peak metamorphic assemblage and therefore is stable to at least ~ 750 °C and 4.0 GPa. The stability of allanite is investigated by means of experimental petrology in the next section.

4. Experimental stability of allanite

4.1. Phase relations

Experiments were carried out in a model composition of subducted crust consisting of K_2O–CaO–MgO–Al_2O_3–SiO_2–H_2O (KCMASH). This is the simplest possible system to form the major phases observed in the eclogites. The starting material was doped with LREE at a 200–300-ppm level and some other trace elements (Table 4). Experimental phase and melting relations in the range 680–1100 °C and 20–45 GPa in this system have been reported by Hermann (2002, in press) and Hermann and Green (2001). Here, these experimental results are examined for unravelling the stability of accessory allanite with respect to the major mineral zoisite. The stability of selected phases and some reactions of these grids are shown in Fig. 4. At the lower pressure, lower temperature end of the investigated grid, zoisite is stable and coexists with kyanite and quartz/coesite and hydrous phases such as biotite, talc, phengite and amphibole. Zoisite occurs as needles of 10–20 μm length (Fig. 5a) and constitutes about 10–25% of the solid phases in the assemblages. Initial breakdown of zoisite is documented by a decrease in its modal abundance and a concomitant increase of brightness in backscattered electron (BSE) images, which results from an increased incorporation of LREE (Fig. 5b). This observation indicates that there is a continuous transition from zoisite as a major mineral to allanite as accessory mineral, which is stabilised due to the presence of the LREE. Zoisite breakdown can be generalised as:

$$\text{Zoisite} + \text{Mg} - \text{phase} \rightarrow \text{clinopyroxene} + \text{kyanite} + \text{allanite} + \text{liquid} \quad (1)$$

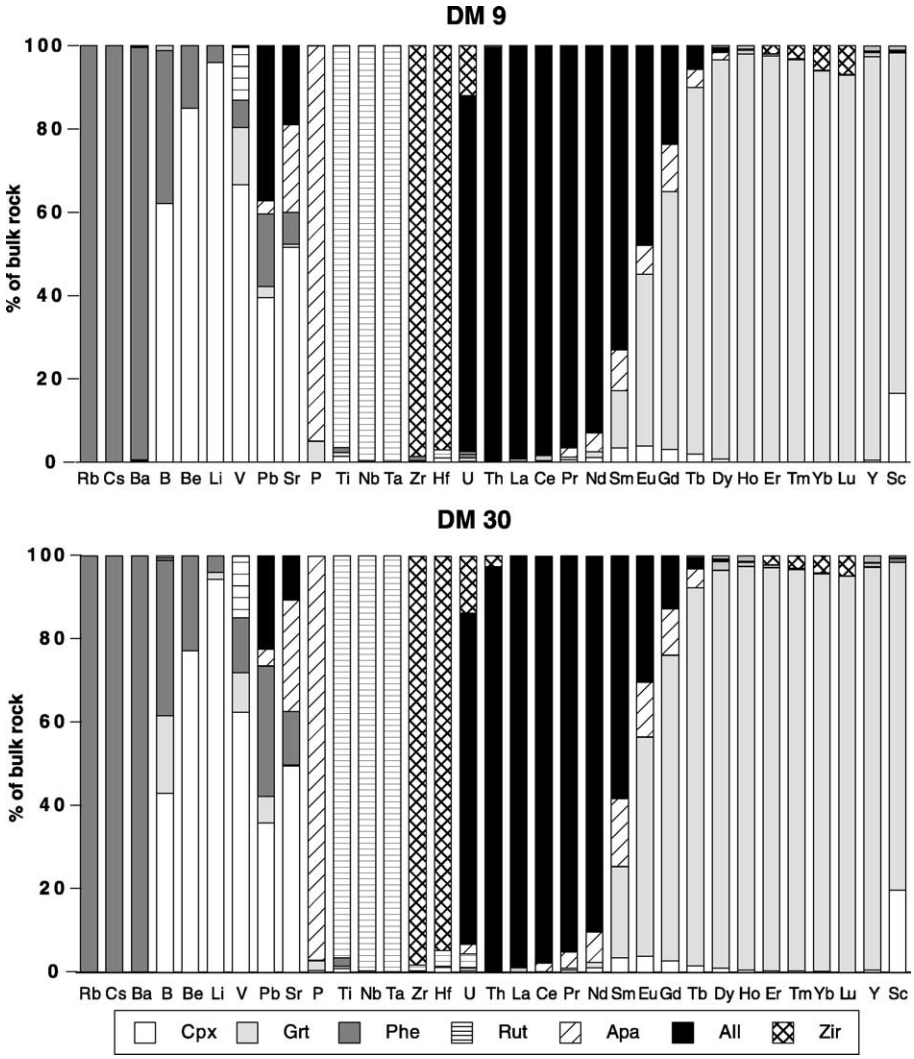

Fig. 3. Trace element distribution among the phases of the eclogites. Significant amounts of trace elements are stored in accessory phases. The following mineral contents were obtained from thin section observations and from mass balance of major and selected trace elements: (a) DM 9: 40% omphacite, 40% garnet, 10% quartz, 6.5% phengite, 2.5% rutile, 0.7% apatite, 0.19% allanite, 0.05% zircon. (b) DM 30: 36% omphacite, 35% garnet, 14% quartz, 12% phengite, 2.5% rutile, 0.52% apatite, 0.1% allanite, 0.032% zircon. Accessory sulfides observed in thin section were not measured and are not considered in the mass balance. The calculated bulk rock composition is generally within 5–15% of the measured values. Considering the variation in the mineral analyses and the analytical uncertainties, this is within error of the applied method. This indicates that no trace element-rich accessory phase has been overlooked in the mass balance. Measured bulk rock Sr is always significantly higher than the value obtained by mass balance. This can either be explained by Sr zoning in apatite and allanite or by introduction of some Sr during the minor retrogression of the eclogites observed in thin section.

Allanite generally forms small 5–10 μm isometric grains and was found to be stable over almost the entire investigated grid. Only the four experiments at the highest temperature were free of allanite. Additionally, in an experiment at 4.5 GPa and 700 °C, allanite was not found. It is not clear yet if this run was beyond the stability of allanite or if allanite was not detected because only very little material was

Table 4
Major and trace element contents of melts and allanite in experimental runs

Sample	P1	C-825	C-983	UHP50		C-896		C-905	C-907	UHP60
		melt	melt	melt	all	melt	all			
T (°C)		950	950	1000		1000		1000	1150	1080
P (kbar)		35	30	45.2		35		30	35	42
Major elements (wt.%)										
SiO_2	61.5	66.45	66.67	63.57	35.12	65.92	35.61	66.17	66.88	65.98
Al_2O_3	21	12.34	12.72	12.36	26.11	12.33	25.76	12.39	13.61	13.40
MgO	8	0.71	0.54	0.41	3.24	0.57	5.01	0.71	1.00	0.53
CaO	6	1.77	1.48	1.21	17.63	2.52	15.14	2.00	4.06	1.57
K_2O	3	8.05	8.49	8.87		6.96		7.17	6.50	10.03
Na_2O	0.2	0.22	0.18	0.39		0.17		0.10	0.21	0.26
H_2O		~ 10	~ 7	~ 9	1.78	~ 7	1.79	~ 6	~ 5	~ 8
Σ TE	0.3	0.44	0.23	0.32	11.69	0.37	14.62	0.36	0.54	0.47
Σ	100	99.98	97.30	96.12	95.57	95.84	97.93	94.90	97.79	99.76
Trace elements (ppm)										
Rb	357	946	580	606	n.a.	728	n.a.	658	808	929
Sr	226	861	304	541	n.a.	425	n.a.	399	537	562
Y	251	25	5.8	7.5	<389	15	3957	11	46	6.6
Zr	271	276	127	222	<475	203	<475	236	457	230
Ba	299	873	422	595	<200	583	<200	521	730	744
La	235	123	151	171	38,182	359	43,917	360	592	534
Ce	283	151	175	209	42,527	416	48,078	415	673	584
Nd	121	60	48	79	11,267	126	15,424	139	234	129
Sm	107	45	12	34	4345	38	5734	54	105	29
Eu	129	53	12	30	n.a.	39	n.a.	72	103	27
Gd	100	25	6	13	3565	14	7374	14	44	10
Yb	136	7.2	1.7	1.9	<208	3.7	333	3.4	15	1.6
Cations (for 12 oxygen + OH)										
Si					3.01		2.99			
Al					2.59		2.55			
Mg					0.41		0.63			
Ca					1.62		1.36			
Σ TE					0.37		0.47			
Σ cat					8.00		8.00			

P1 refers to starting composition of KCMASH experiments. The experiments UHP 50, 60 and C-983 contain only 75% of the trace elements due to dilution with P1c starting material. C-907 and UHP60 do not contain accessory allanite. H_2O contents are estimated from mass balance in glasses (Hermann and Green, 2001) and calculated from stoichiometry in allanite. The sum of trace elements as oxides (Σ TE) is reported, n.a.: not analysed.

recovered from this run. Allanite disappearance is not linked to breakdown of the major phases in the investigated grid. Even major liquid-producing reactions such as talc breakdown, biotite- and phengite-melting do not coincide with the elimination of allanite (Fig. 1). Small amounts of H_2O (2–5%) added to the starting material produced hydrous granitic melts above 800–900 °C (Fig. 4). At lower temperature, the liquid coexisting with the solid phases could not be analysed because it is too water rich to quench to a glass. Mass balance indicates that such a water-rich liquid formed less than 10% of the experimental charge in the lower temperature runs. Allanite was found to be stable with the hydrous unquenchable liquid as well as with the hydrous granitic melt (Fig. 5c). With increasing amount of

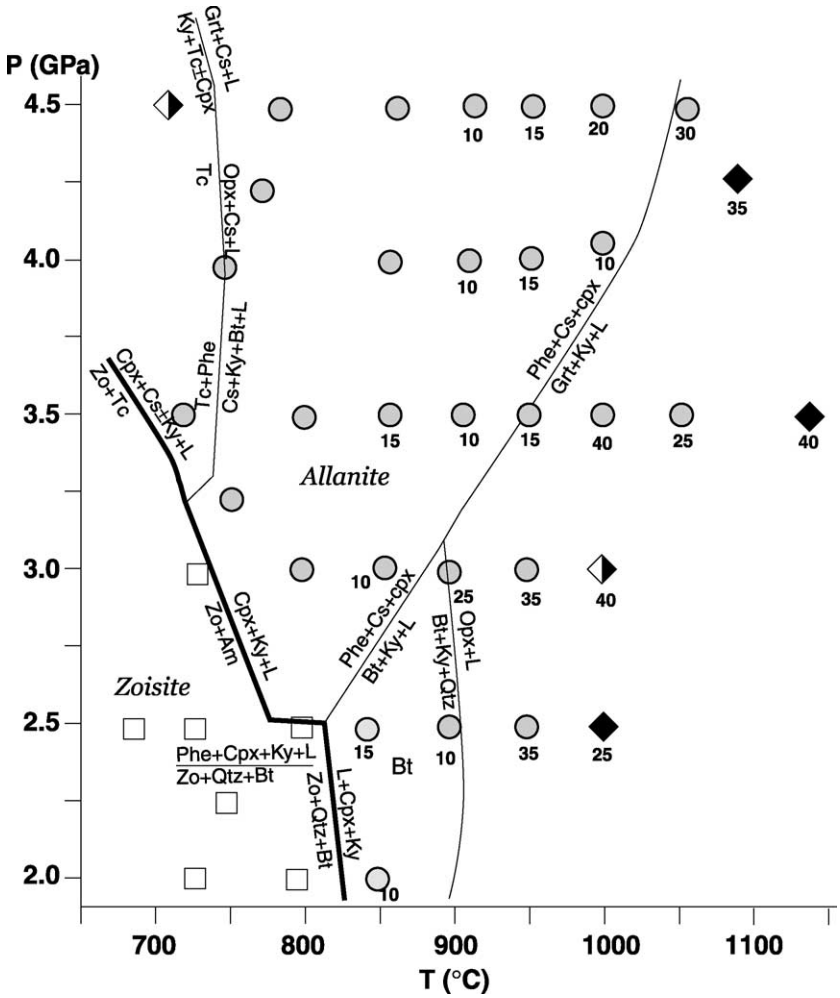

Fig. 4. The experimental stability of zoisite (open squares) and allanite (grey dots) in the KCMASH system according to results reported by Hermann and Green (2001) and Hermann (2002, in press). Diamonds indicate allanite-free experiments. Half-filled diamonds are used for experiments, where allanite was not found in the sectioned capsule but mass balance suggests the presence of allanite. Major dehydration and melting reactions according to Hermann (2002) are given. Numbers below experiments correspond to the estimated amount of partial melt present in the experimental run. In experiments without label, the amount of liquid is <10%. Abbreviations: Cs = coesite, Qtz = quartz, Phe = phengite, Cpx = clinopyroxene, Opx = orthopyroxene, Grt = garnet, Ky = kyanite, Bt = biotite, Tc = Talc, Zo = Zoisite, Am = amphibole, L = liquid.

melt, the number of allanite grains in the sectioned capsule decreased and at the highest temperature investigated, allanite disappeared. These features suggest that the complete consumption of allanite is not related to a breakdown reaction but is a function of dissolution in the melt. Consequently, the stability of allanite is in a first order a function of bulk rock REE content and temperature.

4.2. Mineral composition

Zoisite is close to the ideal formula of $Ca_2Al_3Si_3O_{12}(OH)$ (Fig. 6). The transition from zoisite to allanite is characterised by a continuous decrease of CaO and Al_2O_3 and an increase of MgO and total REE. Most allanites display a weak to strong patchy zoning related to different amounts of LREE incor-

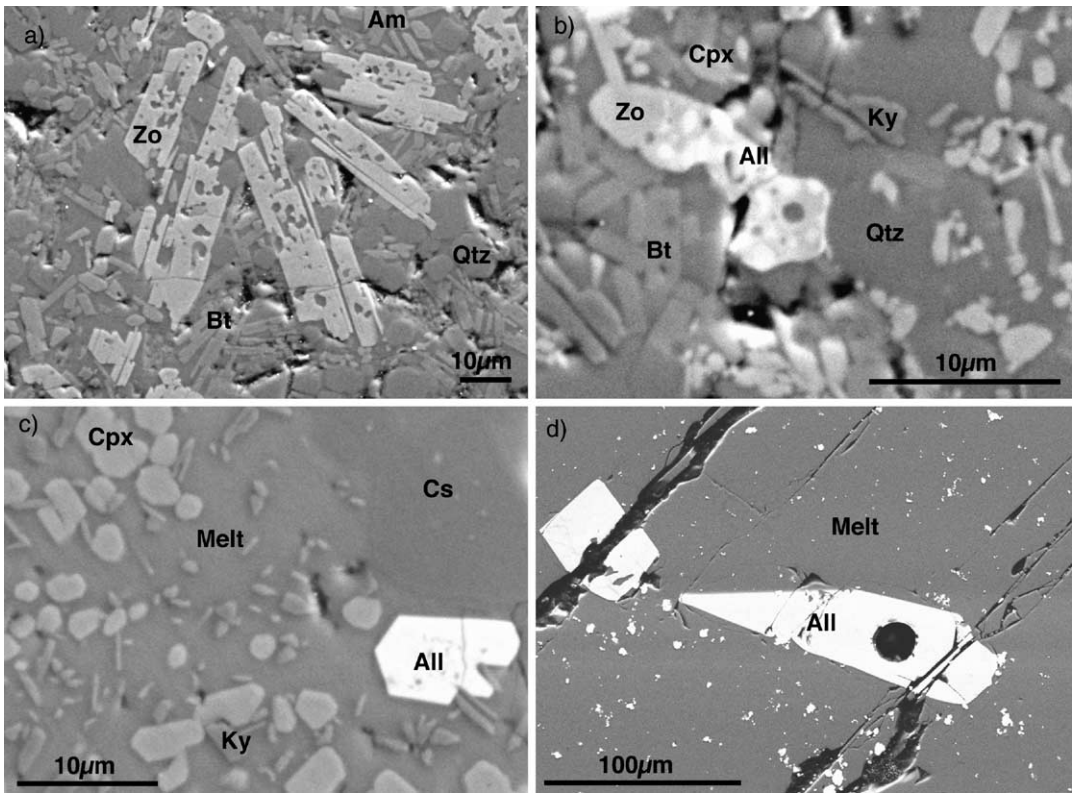

Fig. 5. BSE-images of experimental runs. (a) Zoisite (Zo) is stable at 2.25 GPa, 760 °C (run C-995) and coexists with quartz (Qtz), biotite (Bt) and calcic amphibole (Am). (b) The transition from zoisite to allanite (All) is characterised by an increase in BSE intensity related to the increase of LREE in allanite (run C-988, 2.0 GPa, 850 °C). Other phases present are kyanite (Ky), clinopyroxene (Cpx), biotite and quartz. (c) Idiomorphic allanite is stable with hydrous granitic melt and coesite (Cs) at 3.0 GPa, 950 °C (run C-989). (d) Large homogenous allanite was produced in run C-1245 (2.0 GPa, 900 °C) permitting to determine trace element partitioning. The black spot is the pit of Laser Ablation ICP-MS analysis.

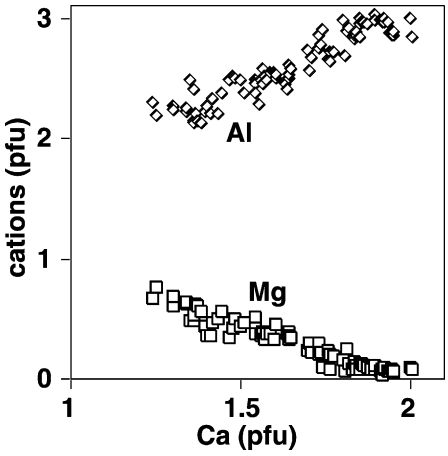

Fig. 6. Range of allanite compositions found in experimental runs (KCMASH system) given in cations per formula unit (pfu) when normalised to Si = 3.

porated. Some large allanites have been analysed with the electron microprobe for LREE. Generally, allanite contains 4–5 wt.% La_2O_3, 5–6 wt.% Ce_2O_3, and 1–2 wt.% Nd_2O_3 and the rest of the trace elements are < 1 wt.% (Table 4). Small allanite has been analysed by SEM EDS and normalised to Si = 3. The slope of Mg versus Ca in cations per formula unit is − 1 and the slope of Al versus Ca is + 1 (Fig. 6). This suggests that in these Fe-free experiments the LREE are incorporated by the coupled exchange Ca + Al ↔ REE + Mg. The natural allanite display low Mg but high Fe contents (Table 2). Thus, the charge balance in natural allanite is mainly maintained by a change in oxidation state of Fe from ferric to ferrous iron according to the exchange $Ca + Fe^{3+} \leftrightarrow REE + Fe^{2+}$.

5. Allanite–melt partitioning

In order to investigate allanite–melt trace element partitioning in a natural system, other experiments were designed. A granodioritic bulk rock composition was chosen, containing about 8.8 wt.% of H_2O and 350–450 ppm of LREE, 475 ppm U and 420 ppm Th (Table 5). Several experiments were run between 2.0 and 3.0 GPa and 700 and 1100 °C. The best results were obtained from an experiment at 2.0 GPa, which was run for 2 h at 1200 °C to completely melt and further homogenise the mix and was then quenched to 900 °C within 5 minutes where it stayed for 320 hours (run C-1245). This experiment produced about 80% of a homogenous hydrous granitic melt. Several 150–250-μm long, 30–60-μm wide needles of euhedral allanite were formed (Fig. 5d), which display only minor zoning (Table 5). These observations indicate that allanite was in equilibrium with the melt. Very small zircons and one big garnet were also found in the melt domain of the experiment. At the bottom end of the capsule, a minor amount of orthopyroxene, amphibole, kyanite and quartz was found.

Table 5
Major and trace element composition of starting material and products of run C-1245 used for determining the trace element partitioning between allanite and melt

	Starting material		Allanite		Melt		*D*
wt. %				SD (10)		SD (7)	
SiO_2	60.2		33.5	0.6	62.47	0.6	0.54
Al_2O_3	14.6		22.9	0.6	13.10	0.1	1.75
FeO	4.11		7.79	0.4	1.29	0.08	6.05
MgO	1.89		1.21	0.12	0.56	0.045	2.15
CaO	2.50		14.65	0.83	1.93	0.08	7.60
Na_2O	2.17				2.30	0.15	
K_2O	2.54				3.51	0.10	
H_2O	8.80		1.95		11.00		
Σ TE	2.11		14.59		0.19		
Total	99.1		96.59		96.15	0.6	
ppm		SD (7)		SD (3)		SD (4)	
P	588	30	345	121	65.6	3.3	5.3
Y	421	10	6772	499	43.1	2.6	157
Zr	21,300	–	<912		160	4	<5.7
Ba	376	5	80	18	411	7	0.19
La	444	12	12,924	900	61.0	3.0	212
Ce	379	11	12,850	938	59.7	2.7	215
Pr	352	10	12,413	1007	58.8	2.0	211
Nd	416	13	12,224	1022	59.7	2.5	205
Sm	381	12	11,342	994	59.0	1.6	192
Eu	352	11	11,900	1753	43.8	0.4	272
Gd	364	11	9632	863	47.8	1.2	201
Dy	381	12	7842	621	39.4	0.9	199
Er	379	12	5587	376	36.3	3.2	154
Yb	400	13	3937	170	38.9	3.4	101
Lu	397	13	3272	154	38.2	2.2	86
Hf	584	55	<62		12.0	0.7	<5.2
Th	421	22	6724	924	110	3	61
U	475	24	3975	141	195	1	20

H_2O contents are estimated from mass balance in the melt and calculated from stoichiometry in allanite. The sum of trace elements as oxides (Σ TE) is also given. The 1σ standard deviation of multiple analyses in % is shown. The number of analyses is given in parenthesis. Zr and Hf in allanite represent maximum values because of slight contamination by zircon. This contamination contributes to less than 5 ppm to the HREE content of allanite and is thus not relevant.

The unusually large size of the allanite made analyses with LA-ICP-MS possible. The resulting allanite and melt compositions and the calculated partitioning are given in Table 5 and shown in Fig. 7. Partition coefficients given here follow the terminology of Beattie et al. (1993) and refer to concentration ratios between two phases. The $D_{LREE}^{all/melt}$ is about 200 and decreases to about 100 for $D_{HREE}^{all/melt}$. $D_{Th}^{all/melt}$ is 61 and $D_{U}^{all/melt}$ is 20, indicating that these elements are strongly enriched in allanite. More importantly, Th and U can be fractionated by allanite as Th is preferentially incorporated. $D_{Ba}^{all/melt}$ is <1 indicating that LILE preferentially enter the melt.

The observed partitioning can be compared with experiments in the KCMASH system, for a limited number of elements and experiments, where REE analyses for melts and allanite are available (Table 4). In experiment UHP 50 and C-896, the partitioning $D_{LREE}^{all/melt}$ is about 220–120. This is very similar to the values obtained from the experiment in the natural composition.

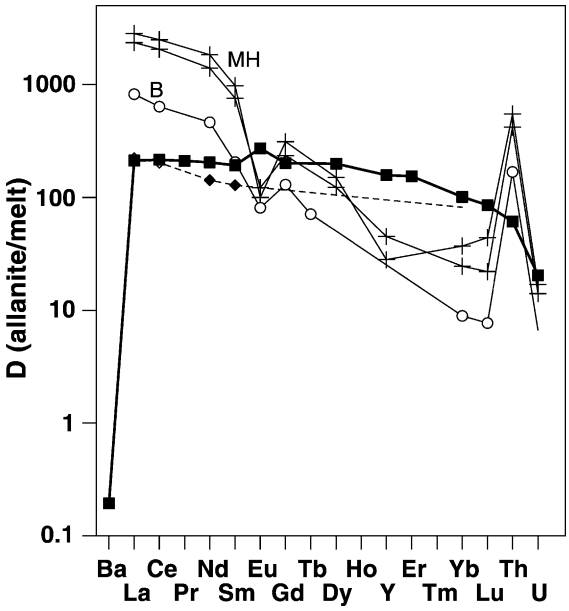

Fig. 7. Experimentally determined partitioning between allanite and hydrous granitic melt in experiment C-1245 (filled squares) at 2.0 GPa, 900 °C. The less precise partitioning from runs UHP 50 and C-896 (see Table 4) is shown in black diamonds and a dotted line. Also indicated are literature values based on allanite–obsidian glass pairs from Mahood and Hildreth (1983; crosses, MH) and Brooks et al. (1981; open dots, B).

6. LREE-saturation of melts

Allanite is able to control the LREE contents of melts because LREE are present at a weight percent level in allanite. Tables 4 and 5 report trace element analyses of melt pools. Allanite is present in experiment C-825, UHP 50, C-983, C-896 and C-1245 and therefore LREE contents of coexisting melts are saturated. Mass balance calculations indicate that C-905 is likely to have some accessory allanite, which was not found in the SEM investigation of the run. C-907 and UHP 60 are allanite free and therefore the measured LREE contents are below saturation. The LREE contents of melts in the KCMASH system increase with increasing temperature but show no clear trend with pressure. The experiment in the natural composition (C-1245) is in agreement with the trend established in the KCMASH melts.

7. Discussion

7.1. Importance of allanite on trace element budget of subducted crust

The two investigated eclogites experienced metamorphic conditions of ~ 730 °C, 4.0 GPa (Schertl et al., 1991; Hermann, in press) and therefore originate from about 120 km depth. Such rocks are unique because they permit insight into subduction zone processes at a critical depth for the formation of arc magmas. The most striking feature of the data (Fig. 3) is the large amount of incompatible trace elements, which are important for characterising subduction zone magmas, incorporated in accessory phases. Allanite makes up only 0.1–0.2% of the rock but contains more than 90% of bulk LREE and Th. Allanite is also the most important host for U (75–80%) and has also the highest Pb and Sr contents of all eclogite minerals. However, because Sr and Pb are also present in the more abundant apatite and especially omphacite, the contribution of allanite to the Pb (25–40%) and Sr (10–20%) is less pronounced than

for Th, and LREE. The importance of allanite for the LREE-budget in an eclogite has been first highlighted by Tribuzio et al. (1996). They found that in an eclogite metamorphosed to ~550 °C, 1.5 GPa, allanite and apatite are the major hosts for LREE, in agreement with the results presented here. In lower metamorphic blueschists and eclogites, lawsonite and epidote are important hosts for LREE (Domanik et al., 1993; Tribuzio et al., 1996; Sassi et al., 2000).

The data presented here demonstrate that accessory phases dominate the Th, U, HFSE, LREE, P-budget in subducted crust (Fig. 3). Therefore, the stability of these minerals as well as partitioning data of these minerals with liquids are fundamental to understand flux of key-elements from the subducted slab to the mantle wedge. In the following section, the role of allanite in the behaviour of LREE and Th is discussed in greater detail.

7.2. Stability of LREE-rich minerals

Trace element analysis of minerals from blueschist to eclogite facies rocks suggested that lawsonite and epidote/zoisite are the main minerals containing LREE in metabasic and metapelitic compositions (Domanik et al., 1993; Tribuzio et al., 1996). The stability of lawsonite and clinozoisite/zoisite in basaltic to andesitic compositions has been investigated experimentally by Poli and Schmidt (1995). They find that clinozoisite/zoisite disappears at pressures above 3.0 GPa while lawsonite is only stable at relatively low temperatures (<650 °C at 3.0 GPa; <750 °C at 5.5 GPa). Combining the information from trace element distributions from natural rocks and experimental results, one is tempted to assume that the breakdown of the hydrous phases such as lawsonite and zoisite might produce LREE-rich fluids. However, the experiments presented here show that this simplification is not justified. The presence of LREE in experiments stabilises accessory allanite as a breakdown product of zoisite. This transition is associated with a decrease of factor 100–500 in modal abundance of the epidote-group mineral from a major to an accessory phase with a concomitant increase in the concentration of the LREE of about the same factor. While such a decrease in epidote abundance liberates H_2O, the LREE are not necessarily released. Therefore, liberation of trace elements cannot be deduced from stability fields of major minerals only. In this study, breakdown of allanite was not correlated with breakdown of any major phase. Rather, there is a continuous dissolution of allanite in the presence of a liquid phase. In the next section, it will be evaluated how long allanite can survive partial melting of subducted crustal material.

7.3. Allanite presence during partial melting?

The dissolution of allanite depends on the solubility of LREE in a coexisting liquid. Studies on the LREE saturation of melts buffered with monazite demonstrated that temperature and melt composition are the two main factors that determine the LREE saturation of melts, while pressure is much less important (Rapp and Watson, 1986; Montel, 1993). These studies also showed that for a similar melt composition, there is a linear trend between inverse temperature and logarithm of the REE concentration in the melt. In a plot of ln Ce content versus inverse temperature, the melts in equilibrium with allanite define a linear trend (Fig. 8a, squares). Because the temperature spread of the experiments is only 100 °C, the trend is not very well constrained. The trend can be compared to saturation levels of hydrous granitic melts with similar water contents and composition buffered by monazite established at higher temperatures (Rapp and Watson, 1986). Although the monazite dissolution experiments were conducted at much lower pressures (0.8 GPa) and in a slightly more silica-rich melt composition, the two sets of experiments agree well. This further supports the hypothesis that temperature is the principal controlling factor on LREE saturation of melts (Montel, 1993). The slight differences in composition (within granitic melts), the slightly different water contents (5–10%), different pressures and the nature of the LREE-rich phase (monazite or allanite) controlling the melt composition seem to have less influence on the LREE saturation level. The combined data set from monazite and allanite permits estimation of LREE saturation levels at lower temperature using a linear extrapolation (Fig. 8a). Using this extrapolation, Ce contents of liquids would be 22 ppm at 800 °C and only 4 ppm at 700 °C. The Ce contents of the experiments at 1080 and 1150 °C are situated below the saturation line in agreement with the absence of allanite in these experiments.

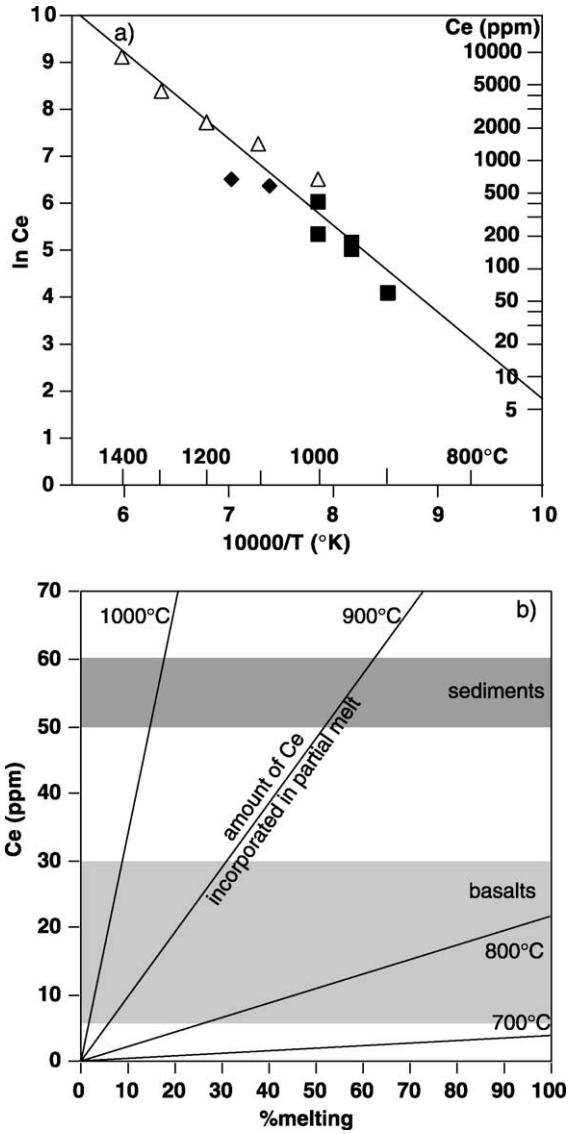

Fig. 8. (a) Experimental data on LREE saturation of granitic melts. Experiments with allanite present are shown with filled squares (this study). Triangles stand for monazite-controlled hydrous melts according to the experiments by Rapp and Watson (1986). The Ce contents of melts without allanite (filled diamonds) are situated below the least square linear fit of the saturation level. (b) Solid lines represent the amount of Ce incorporated in partial melts as a function of temperature and degree of melting. The range of Ce contents for basalts and oceanic sediments is shown with grey bars. If the Ce-capacity of the partial melt is lower than the available Ce in bulk rock, allanite is likely to be a residual phase.

LREE contents of liquids also change with the liquid composition (Montel, 1993). The liquids in the experiments are hydrous granitic melts, which are in equilibrium with a typical residue of subduction zone rocks and are likely to be close to the composition of subduction zone liquids (Hermann and Green, 2001). Therefore, the values shown in Fig. 8a represent a good approximation to Ce contents of subduction zone liquids. The Ce content of liquids can now be combined with bulk rock Ce contents to evaluate how much partial melting is needed to completely accommodate the Ce in the liquid phase. Bulk rock basaltic crust ranges from 6 to 30 ppm Ce (Schilling et al., 1983), whereas sediments have a higher Ce content on average of about 50–60 ppm (Plank and Langmuir, 1998). At 700 °C, the Ce content of the liquid is too low to completely accommodate bulk rock Ce contents for basalts and sediments. If partial melting does not exceed 20% at 800 °C, LREE-rich phases such as allanite are to be expected in the residue (Fig. 8b). At 900 °C, allanite might be consumed in mafic rocks with low Ce contents that experience more than 5–10% partial melting. However, for sediments and basalts with higher Ce contents, allanite survives significant amounts of partial melting and is still the most important host for LREE. At 1000 °C, less than 10% of partial melting is enough to dissolve the LREE out of the mafic rocks, but due to the higher bulk rock LREE content, allanite is still expected in the sediments. These calculations demonstrate that allanite is expected to be present during initial stages of partial melting to at least 900 °C in subducted oceanic crust.

7.4. Allanite–melt partitioning

Because allanite can coexist with melt to at least 900 °C, knowing the allanite–melt partitioning is important for establishing the trace element characteristics of subduction zone liquids. The data in Table 5 and Fig. 7 represent the first experimentally determined trace element partitioning between a likely subduction zone melt and allanite. It shows very high $D_{\mathrm{LREE}}^{\mathrm{all/melt}}$ of about 200 and $D_{\mathrm{Th}}^{\mathrm{all/melt}}$ of about 60 at 2.0 GPa, 900 °C.

Trace element partition coefficients derived from allanite phenocrysts in rhyolitic glass (Brooks et al., 1981; Mahood and Hildreth, 1983) have similar features as the experiments, with LREE and Th preferen-

tially incorporated in allanite. However, the patterns differ significantly with the phenocryst–melt pairs showing much higher values in $D_{LREE}^{all/melt}$ and $D_{Th}^{all/melt}$, while the $D_{HREE}^{all/melt}$ values are lower than those determined experimentally (Fig. 7). There are several possible reasons for these differences. Firstly, the techniques employed to determine the partitioning are completely different. Secondly, the melt compositions are different: rhyolite is more silica rich and slightly more peraluminous than the granodioritic glass used in the experiments. Thirdly, the Mahood and Hildreth (1983) results may be applicable at lower temperature (720–760 °C estimated for the lava). While it is not possible with the existing data to evaluate the influence of melt compositions on partitioning the effect of temperature can be semi-quantitatively evaluated.

Similar to LREE in monazite and Zr in zircon, LREE in allanite are major and not trace elements. The amount of Ce in allanite is always on the order of 1.2–6 wt.%, i.e. it varies about a factor 5. On the other hand, the Ce content in the melts can change orders of magnitude with temperature (Fig. 8a). Therefore, the LREE partitioning between allanite and melt is mainly driven by the LREE-saturation level of the melt, which in turn is a function mainly of temperature. If we take the measured Ce contents of about 52,000 ppm of the allanite in the eclogite (Table 3) and an extrapolated Ce content in the melt of 6.7 ppm at 730 °C (Fig. 8a), the estimated peak metamorphic temperature, the resulting partitioning is about 7800. This value is much closer to the LREE partitioning data given by Mahood and Hildreth (1983).

7.5. Implications for subduction zone magmatism

Because allanite strongly prefers LREE and Th with respect to liquid, the presence of allanite during dehydration/partial melting in subducted crust has a profound influence on the LREE and Th/U pattern of liquids produced in the subducted oceanic crust. On the basis of detailed geochemical studies, it has been suggested that enrichment in LREE with respect to HFSE in arc lavas reflects addition of a "subduction component" (McCulloch and Gamble, 1991; Pearce and Peate, 1995). These studies also show that the LREE enrichment is always lower than the LILE enrichment. The trace element distributions in the deeply subducted eclogite (Fig. 3) demonstrate that allanite and phengite host most of the LILE, LREE, and Th. This study shows that for the temperature range from 600 to 950 °C, which is crucial for subduction zone liquid extraction, allanite does not disappear along a reaction but is continuously dissolved if a liquid is present. Experimental studies on the stability of phengite show that at 950 °C phengite is stable over a wide range of pressures and compositions (Domanik and Holloway, 2000; Hermann and Green, 2001). Thus, like the LREE, the LILE are not released by the breakdown of its host phase phengite, but by the interaction of phengite with liquids.

In the following, the control of phengite and allanite on the trace element composition of subduction zone liquids at two different temperatures is discussed. At 950 °C, the liquid is a hydrous granitic melt (Hermann and Green, 2001). In contrast, at 600 °C, the liquid is likely to be supercritical and probably contains similar amounts of dissolved species and H_2O (Hermann, in press) and will be named "fluid" hereafter. The bulk partitioning between solid and liquid determines whether an element is preferentially incorporated in the liquid or if it stays in the residual solids. The bulk partitioning for an element represents the sum of the abundances of each mineral multiplied by $D_{element}^{mineral/liquid}$. In the case of LREE and LILE, the bulk partitioning is almost completely controlled by allanite and phengite, respectively. Consequently, the abundance of phengite and allanite in subducted rocks and their partitioning with a liquid will determine, to a first order, the ratios and abundance of these key elements in the liquid leaving the subducting slab.

For a fluid at ~ 600 °C, Ba partitioning between phengite and liquid is likely to be between 1 and 10 (Zack et al., 2001). Thus, if the subducted oceanic crust (basalts + sediments) contain 1–10% of phengite, the bulk partitioning is likely to be in the order of 0.01–1. $D_{LREE}^{all/fluid}$ is estimated to be ~ 100,000 at this temperature using the approach described above. For the given ranges of LREE bulk compositions in basalts and sediments (Fig. 8), there is between 0.01% and 0.1% allanite in the rocks, resulting in a $D_{LREE}^{bulk/fluid}$ of 10–100. The LREE are therefore compatible in the residue and not easily released. A Ce content of about 0.43 ppm of the fluid can be estimated on the basis of the extrapolation of the experimental data on Ce-solubility in saturated liquids (Fig. 8a). Therefore, such a fluid would be

characterised by low LREE contents and high LILE/LREE ratio of about 100. At a temperature of 950 °C, the amount of Ce in a hydrous granitic melt is about 180 ppm (Fig. 8a), much higher than for the lower temperature fluid, and the partitioning $D_{LREE}^{all/fluid}$ is about 200. Using the same approach as above, the bulk LREE partitioning is estimated to be in the range of 0.02–0.2. LREE are thus incompatible in the residue and preferentially enter the melt. At 950 °C, 3.5 GPa, Hermann and Green (2001) determined the $D_{Ba}^{phe/melt}$ to be ~ 1.2 resulting in a $D_{Ba}^{bulk/melt}$ of about 0.01–0.1. The liquid leaving the subducted slab at 950 °C is thus a hydrous granitic melt characterised by much higher amounts of LREE and lower LILE/LREE ratio than the lower temperature fluids at 600 °C.

The constraints on the subduction zone liquid presented here on the basis of experiments and geochemistry of eclogites agree very well with observations on arc lavas. Lavas with high LILE/LREE ratios do not show significant enrichment of LREE with respect to HREE indicating that the metasomatic agent was a fluid with overall low LREE and high LILE abundances (Pearce and Peate, 1995; Elliott et al., 1997; Hawkesworth et al., 1997). On the other hand, mantle source enrichment of LREE and other fluid immobile elements such as Th is associated with smaller LILE/LREE ratios and has been associated to a "subduction melt" component (Elliott et al., 1997; Hawkesworth et al., 1997; Pearce and Peate, 1995).

Another important feature of the "fluid component" in arc lavas are low Th/U ratios (Elliott et al., 1997; Hawkesworth et al., 1997). Th/U disequilibrium dating provides evidence that Th and U are fractionated about 30–120 ka prior to arc lava emplacement (Hawkesworth et al., 1997). This strongly suggests that Th–U fractionation occurs during liquid extraction in the down-going slab and cannot be related to a change in bulk rock Th/U during hydrothermal alteration at the ocean floor (Hawkesworth et al., 1997). In the investigated eclogites, nearly all Th and a major part of the U is hosted in allanite. U and Th partitioning between allanite and melt demonstrate that Th is preferred to U in allanite. Therefore, residual allanite could partly be responsible for the generation of fluids with low Th/U ratios. As with the LREE, it is expected that the Th content of a melt coexisting with allanite is strongly dependent on temperature. Therefore, significant Th release will only occur at high temperatures. This is in agreement with geochemical data from arc rocks, indicating that significant transfer of Th from the slab to the mantle wedge is always associated with a "sediment melt component" (Elliott et al., 1997; Hawkesworth et al., 1997).

8. Conclusions

(1) Accessory minerals play an important role in the trace element budget of subducted crust. In two eclogites from the Dora-Maira massif, which experienced metamorphic conditions of ~ 4.0 GPa, 730 °C, more than 95% of Ti, Nb and Ta is incorporated in rutile, more than 95% of Zr and Hf is incorporated in zircon and more than 90% of LREE and Th is incorporated in allanite. Allanite and zircon host nearly all U and P is mainly stored in apatite. Among the major minerals, phengite is the most interesting one because it incorporates more than 95% of the bulk rock Rb, Ba and Cs.

(2) Piston cylinder experiments demonstrate that allanite is expected as a residual phase in subducted crust in the region of liquid extraction. Therefore, allanite will control the LREE and the Th content of subduction zone liquids.

(3) On the basis of experiments, LREE saturation levels of subduction zone liquids coexisting with allanite are estimated to be 1/4 the primitive mantle value at 600 °C, 12 times at 800 °C and 180 times at 1000 °C. This demonstrates that significant LREE (and Th) mantle metasomatism is only possible if the subduction zone liquid is extracted at high temperature.

(4) Residual allanite and phengite in the subducted rocks control the composition of the subduction zone liquid. This liquid is probably a supercritical fluid at low temperature, characterised by low LREE contents and a high LILE/LREE ratio and a hydrous granitic melt at high temperature, characterised by higher LREE contents and a lower LILE/LREE ratio.

(5) Experimentally determined partitioning reveal that $D_{Th}^{all/melt} > D_{U}^{all/melt}$. Therefore, residual allanite could participate in the production of subduction zone liquids with low Th/U ratios.

Acknowledgements

I would like to thank W.O. Hibberson and D. Scott for technical assistance in the high-pressure laboratory, the crew from the Electron Microscopy Unit (ANU) for help with the SEM, and C. Allen and M. Shelley for their assistance at the laser ablation ICP-MS. Comments of D. Rubatto and C. Spandler and careful reviews of R. Tribuzio and T. Zack helped to improve the paper. The editorial handling by R. Rudnick is acknowledged. This work was financially supported by the Schweizerischer Nationalfonds and the Australian Research Council. **[RR]**

References

Beattie, P., Drake, M., Jones, J., Leeman, W., Longhi, J., McKay, G., Nielsen, R., Palme, H., Shaw, D., Takahashi, E., Watson, B., 1993. Terminology for trace element partitioning. Geochim. Cosmochim. Acta 57, 1605–1606.

Brooks, C.K., Henderson, P., Rønsbo, J.G., 1981. Rare-earth partition between allanite and glass in the obsidian of Sandy Braes, Northern Ireland. Mineral. Mag. 44, 157–160.

Carswell, D.A., Wilson, R.N., Zhai, M., 2000. Metamorphic evolution, mineral chemistry and thermobarometry of schists and orthogneisses hosting ultra-high pressure eclogites in the Dabieshan of central China. Lithos 52, 121–155.

Domanik, K.J., Holloway, J.R., 2000. Experimental synthesis and phase relations of phengitic muscovite from 6.5 to 11 GPa in a calcareous metapelite from the Dabie Mountains, China. Lithos 52, 51–77.

Domanik, K.J., Hervig, R.L., Peacock, S.M., 1993. Beryllium and boron in subduction zone minerals: an ion microprobe study. Geochim. Cosmochim. Acta 57, 4997–5010.

Eggins, S.M., Rudnick, R.L., McDonough, W.F., 1998. The composition of peridotites and their minerals: a laser ablation ICP-MS study. Earth Planet. Sci. Lett. 154, 53–71.

Elliott, T., Plank, T., Zindler, A., White, W., Bourdon, B., 1997. Element transport from slab to volcanic front at the Mariana arc. J. Geophys. Res. 102, 14991–15019.

Exeley, R.A., 1980. Microprobe studies on REE-rich accessory minerals; implications for Skye granite petrogenesis and REE mobility in hydrothermal systems. Earth Planet. Sci. Lett. 48, 97–110.

Gromet, L.P., Silver, L.T., 1983. Rare earth element distributions among minerals in a granodiorite and their petrogenetic implications. Geochim. Cosmochim. Acta 47, 925–940.

Hawkesworth, C., Turner, S., Peate, D., McDermot, F., Calsteren, V., 1997. Elemental U and Th variations in island arc rocks: implications for U-series isotopes. Chem. Geol. 139, 207–221.

Hermann, J., 2002. Experimental constraints on phase relations in subducted continental crust. Contrib. Mineral. Petrol. 143, 219–235.

Hermann, J., in press. Experimental evidence for diamond-facies metamorphism in the Dora-Maira massif. Lithos.

Hermann, J., Green, D.H., 2001. Experimental constraints on high pressure melting in subducted crust. Earth Planet. Sci. Lett. 188, 149–168.

Luth, W.C., Ingamells, O., 1965. Gel preparation of starting materials for hydrothermal experimentation. Am. Mineral. 50, 255–258.

Mahood, G., Hildreth, W., 1983. Large partition coefficients for trace elements in high-silica rhyolites. Geochim. Cosmochim. Acta 47, 11–30.

McCulloch, M.T., Gamble, J.A., 1991. Geochemical and geodynamical constraints on subduction zone magmatism. Earth Planet. Sci. Lett. 102, 358–374.

Montel, J.-M., 1993. A model for monazite/melt equilibrium and application to the generation of granitic magmas. Chem. Geol. 110, 127–146.

Pearce, J.A., Peate, D.W., 1995. Tectonic implications of the composition of volcanic arc magmas. Annu. Rev. Earth Planet. Sci. 23, 251–285.

Pearce, N.J.G., Perkins, W.T., Westgate, J.A., Gorton, M.P., Jackson, S.E., Neal, C.R., Chenery, S.P., 1997. A compilation of new and published major and trace element data for NIST SRM 610 and NIST SRM 612 glass reference materials. Geostand. Newsl. 21, 115–144.

Plank, T., Langmuir, C.H., 1998. The chemical composition of subducting sediments and its consequences for the crust and mantle. Chem. Geol. 145, 325–394.

Poli, S., Schmidt, M.W., 1995. H_2O transport and release in subduction zones: experimental constraints on basaltic and andesitic systems. J. Geophys. Res. 100, 22299–23314.

Rapp, R.P., Watson, B.E., 1986. Monazite solubility and dissolution kinetics: implications for the thorium and light rare earth chemistry of felsic magmas. Contrib. Mineral. Petrol. 94, 304–316.

Rudnick, R.L., Barth, M., Horn, I., McDonough, W.F., 2000. Rutile-bearing refractory eclogites; missing link between continents and depleted mantle. Science 287, 278–281.

Sassi, R., Harte, B., Carswell, D.A., Yujing, H., 2000. Trace element distribution in Central Dabie eclogites. Contrib. Mineral. Petrol. 139, 298–315.

Sawka, W.N., Chappell, B.W., Norrish, K., 1984. Light-rare-earth-element zoning in sphene and allanite during granitoid fractionation. Geology 12, 131–134.

Schertl, H.-P., Schreyer, W., Chopin, C., 1991. The pyrope-coesite rocks and their country rocks at Parigi, Dora Maira massif, Western Alps: detailed petrography, mineral chemistry and PT path. Contrib. Mineral. Petrol. 108, 1–21.

Schilling, J.G., Zajac, M., Evans, R., Johnston, T., White, W., Devine, J.D., Kingsley, R., 1983. Petrologic and geochemical variations along the Mid-Atlantic ridge from 27°N to 73°N. Am. J. Sci. 283, 510–586.

Sorensen, S.S., 1991. Petrogenetic significance of zoned allanite in garnet amphibolites from a paleo-subduction zone: Catalina Schist, southern California. Am. Mineral. 76, 589–601.

Sorenson, S.S., Grossman, J.N., Perfit, M.R., 1997. Phengite-hosted LILE enrichment in eclogite and related rocks: implications for

fluid-mediated mass transfer in subduction zones and arc magma genesis. J. Petrol. 38, 3–34.

Sun, S.S., McDonough, W.F., 1989. Chemical and isotopic systematics of oceanic basalts: implications for mantle composition and processes. In: Sanders, A.D., Norry, M.J. (Eds.), Magmatism in the Ocean Basins. Geological Society Special Publication, London, pp. 313–345.

Tribuzio, R., Messiga, B., Vannucci, R., Bottazzi, P., 1996. Rare earth element redistribution during high-pressure low-temperature metamorphism in ophiolitic Fe-gabbros (Liguria, northwestern Italy): implications for light REE mobility in subduction zones. Geology 24, 711–714.

Zack, T., Rivers, T., Foley, S.F., 2001. Cs–Rb–Ba systematics in phengite and amphibole: an assessment of fluid mobility at 2.0 GPa in eclogites from Trescolmen, Central Alps. Contrib. Mineral. Petrol. 140, 651–669.

Zack, T., Kronz, A., Rivers, T., Foley, S.F., 2002. Trace element abundances in rutiles from eclogites and associated garnet mica schists. Chem. Geol. 184, 97–122.